

Channel Capacity and Bounds In Mixed Gaussian-Impulsive Noise

Tianfu Qi, Jun Wang, *Senior Member, IEEE*, Qihang Peng, *Member, IEEE*,
 Xiaoping Li, *Member, IEEE*, Xiaonan Chen, *Student Member, IEEE*

Abstract

Communication systems suffer from the mixed noise consisting of both non-Gaussian impulsive noise (IN) and white Gaussian noise (WGN) in many practical applications. However, there is little literature about the channel capacity under mixed noise. In this paper, we prove the existence of the capacity under p -th moment constraint and show that there are only finite mass points in the capacity-achieving distribution. Moreover, we provide lower and upper capacity bounds with closed forms. It is shown that the lower bounds can degenerate to the well-known Shannon formula under special scenarios. In addition, the capacity for specific modulations and the corresponding lower bounds are discussed. Numerical results reveal that the capacity decreases when the impulsiveness of the mixed noise becomes dominant and the obtained capacity bounds are shown to be very tight.

Index Terms

Mixed noise, channel capacity, capacity bound, relative entropy

Tianfu Qi, Jun Wang, Xiaonan Chen are with the National Key Laboratory of Wireless Communications, University of Electronic Science and Technology of China, Chengdu 611731, China (e-mail: 202311220634@std.uestc.edu.cn).

Xiaoping Li is with the School of Mathematical Sciences, University of Electronic Science and Technology of China, Chengdu 611731, China (e-mail: lixiaoping.math@uestc.edu.cn).

Qihang Peng is with the School of Information and Communication Engineering, University of Electronic Science and Technology of China, Chengdu 611731, China (e-mail: anniepqh@uestc.edu.cn).

I. INTRODUCTION

Characterized by an extremely short duration with large power, impulsive noise (IN) exists in many practical scenarios such as LTE in urban environments [1], wireless digital video broadcasting terrestrial (DVB-T), lightning, underwater acoustic systems [2], wide-band power line systems [3], etc. The most popular model to describe IN is symmetric α stable ($S\alpha S$) distribution which is discussed explicitly in [4]. However, $S\alpha S$ distribution has no general closed-form probability density function (PDF). In practice, due to the Brownian motion of electrons, there always exists white Gaussian noise (WGN) in communication systems. Therefore, IN and WGN together generate the mixed noise.

Capacity is one of the most important performance metric of channel, which represents the ability to transfer error-free information between the communication transmitter and the receiver. The well-known channel capacity under WGN was proposed by Shannon [5]. Subsequently, the capacities of many other channels with different constrains have been analysed. For instance, Abou-Faycal et al. systematically study the capacity of memoryless Rayleigh fading channels in [6] and give the amplitude's characteristic of the capacity-achieving input distribution. Hui Li et al. prove the existence and uniqueness of capacity of the additive inverse Gaussian noise channel, and propose tight closed-form capacity bounds [7]. In [8], Lapidoth and Moser raise a general capacity upper bound based on the dual expression of capacity, based on which numerical lower and upper bounds for several scenarios such as free-space optical intensity channel and Poisson channel are derived [9, 10]. The capacity of communication under $S\alpha S$ noise is calculated by the BA-algorithm [11] and its theoretical analysis is provided in [12]. However, the capacity of mixed noise channels is barely discussed in the existing literature.

Further, for power-limited communication systems, the modulation order could not be infinite and there is a capacity limitation concerning the order. Thus, capacity under a specific modulation scheme is valuable for practical applications. Meilin He et al. present the capacity bounds of M-PAM modulation and the corresponding numerical calculation procedure [13] under WGN channel. However, there is no analytical or general capacity expression. In [14], the capacity of M-ary differential chaos shift keying modulation under WGN channel is analyzed, and explicit capacity bounds are provided. Pei Yang et al. develop a recurrence formula to construct series representation as a numerically efficient way to obtain the capacity bound of Nakagami- m fading channel for BPSK and QPSK modulations [15].

Compared with the model for IN, the model for mixed noise channel is more complicated, which makes the capacity difficult to discuss and different from the capacity based on other noise models such as $S\alpha S$ distribution, Cauchy distribution, etc. In this paper, we analyze the capacity of mixed noise channel as well as its performance with respect to the modulation format for communication systems. The main contributions of this paper are summarized in the following.

- 1) The capacity and numerical bounds of the mixed noise channel are first investigated in the paper. With the statistical properties of the mixed noise model, we analyzed the existence and uniqueness of the capacity under the p -th moment constraints. Then, the features of the optimal input distribution, including the size of the support and the conditions that the optimal input should satisfy, are derived.
- 2) With the simplified mixed noise model, we derive the lower and upper bounds of the capacity based on the mutual information and relative entropy, respectively. Meanwhile, we present the numerical results of the channel capacity with Blabut-Arimoto (BA) algorithm and gradient descent. Results show that the capacity of the mixed noise is lower than that of the Gaussian channel, especially when the impulsivity of the noise is larger. The numerical capacity and the capacity bounds are compared under various scenarios to validate the theoretical deviations.
- 3) For practical applications, the capacity under PAM modulation is discussed, and two lower bounds based on the Hermite quadrature and Fano's inequality are given. Compared with the capacity without modulation order constraint, there is a capacity limit as the signal-to-noise ratio (SNR) increases and the lower bounds are tight with different noise parameters.

The remainder of this paper is organized as follows. In Section II, we provide the mixed noise model and some important properties that will be utilized in the following analysis. In Section III, we formulate and analyze the capacity of mixed noise model with power constraints. Section IV and Section V provide closed-form lower and upper bounds of the capacity, respectively. In Section VI, the capacity related to PAM scheme is analyzed. Numerical results and corresponding applications are described in Section VII. Finally, the paper is concluded in Section VIII.

II. MIXED NOISE MODEL

We consider the communication problem under the memoryless additive mixed noise channel in this paper. The system model can be given as

$$Y = X + N_m, \tag{1}$$

$$N_m = N_s + N_g, \tag{2}$$

where N_m , N_s and N_g represent the random variables (RVs) of the mixed noise, IN and WGN, respectively. N_s and N_g are mutually independent, and Y and X are the received and transmitted signal RVs, respectively. Note that we omit the time index as the considered channel is memoryless.

The IN can be well described by the α stable distribution [16]. α stable distribution is a heavy-tail distribution, and it is denoted as $S(\alpha, \beta, \gamma, w)$, where α , β , γ and w denote the characteristic parameter, skewness parameter, scale parameter and position parameter, respectively. For convenience, we use $N_s \sim$

$S(\alpha, \beta, \gamma, w)$ to denote that N_s follows α stable distribution. α stable distribution has no general closed-form PDF, except Gaussian distribution for $\alpha = 2$ and Cauchy distribution for $\alpha = 1$ [16]. Under communication scenarios, the IN is usually distributed symmetrically about zero, i.e., $\beta = w = 0$. Due to the lack of the simple PDF of $S\alpha S$ distribution, it is more difficult to model the mixed noise. Sureka et al. propose an approximated PDF for mixed noise and the model is shown as follows [17],

$$f_{N_m}(n) = \frac{g_0}{I} \left[c_1 e^{-\frac{n^2}{4\gamma_{sg}}} + \frac{c_2(1-c_1)}{|n|^{\alpha+1} + c_2} \right], \quad (3)$$

where

$$c_2 = \frac{\alpha\gamma_s C_\alpha}{g_0(1-c_1)}, \quad (4)$$

$$g_0 = \frac{1}{\pi} \sqrt{\frac{2^{-\frac{1}{2}-\frac{1}{\alpha}} \sqrt{\pi}}{\alpha(\gamma_s^\alpha + \gamma_g)}} \Gamma\left(\frac{1}{\alpha}\right), \quad (5)$$

$$C_\alpha = \frac{1}{\pi} \Gamma(\alpha) \sin\left(\frac{\alpha\pi}{2}\right), \quad (6)$$

$$I = 2c_1 g_0 \sqrt{\pi\gamma_{sg}} + 2g_0(1-c_1)c_2^{\frac{1}{\alpha+1}} \Gamma\left(\frac{\alpha}{\alpha+1}\right) \Gamma\left(\frac{\alpha+2}{\alpha+1}\right), \quad (7)$$

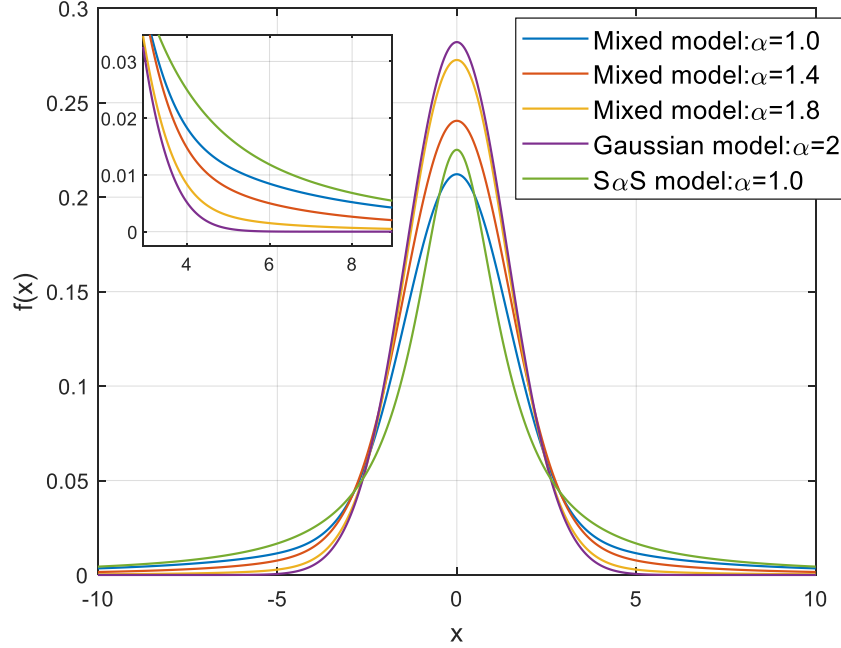
and $\Gamma(a) = \int_0^{+\infty} t^{a-1} e^{-t} dt$. The distribution includes 5 parameters which are $0 < \alpha \leq 2$, $\gamma_s > 0$, $\gamma_g > 0$, $0 \leq c_1 \leq 1$ and $\gamma_{sg} > 0$. α is the characteristic parameter describing the thickness of the tail of the distribution, which is the identical parameter in $S\alpha S$ distribution. γ_g and γ_s are the scale parameters of WGN and IN, respectively. c_1 can be considered as a weight factor, and the distribution will degenerate to Gaussian distribution when $c_1 = 1$. γ_{sg} is a regulatory factor for the main lobe of this distribution. Note that the 5 parameters can be well estimated based on the methods presented in [17]. We present the PDF comparison to facilitate understanding the properties of mixed noise model.

Here, we fix $c_1 = 0.8$, $\gamma_{sg} = \gamma_s = \gamma_g = 1$. We can see that the tail becomes heavier if α is smaller, which is similar to $S\alpha S$ distribution. However, the $S\alpha S$ distribution with the same α has heavier tail since it omit the influence of WGN. Note that we set $\gamma_s = \sqrt{2}$ for $S\alpha S$ distribution to assure the same noise power with the mixed noise. Meanwhile, the PDF of the Gaussian distribution decays quite quickly and can be neglected when $x > 6$ in Fig. 1. Subsequently, we give some important properties of the mixed noise model which will be utilized in what follows.

Property 1: $f_{N_m}(n)$ is continuous and $f_{N_m}(n) \leq g_0/I$.

This property is quite straightforward because of the monotonicity of PDF. To obtain property 2, we first provide an elementary integration formula [18],

$$\int \frac{x^p}{x^{\alpha+1} + c_2} dx = \frac{G(x; \alpha, p, c_2)}{c_2(1+p)}. \quad (8)$$


 Fig. 1: The PDF comparison with different α

In (8), $G(x; \alpha, p, c_2)$ is expressed as

$$G(x; \alpha, p, c_2) = x^{p+1} H_g \left(1, \frac{p+1}{\alpha+1}, 1 + \frac{p+1}{\alpha+1}, -\frac{x^{\alpha+1}}{c_2} \right), \quad (9)$$

where $H_g(\cdot)$ is Gaussian hypergeometric function.

Property 2: N_m has no limited variance but finite p -th moment ($0 < p < \alpha \leq 2$) and can be expressed as

$$\mathbb{E}[|N_m|^p] = 2^{p+1} \gamma_{sg}^{\frac{p+1}{2}} \frac{c_1 g_0}{I} \Gamma \left(\frac{p+1}{2} \right) + \frac{2\alpha \gamma_s C_\alpha G(+\infty; \alpha, p, c_2)}{c_2(p+1)I}, \quad (10)$$

where $\mathbb{E}[X]$ is the mean of X . Note that $G(+\infty; \alpha, p, c_2)$ is finite since the p -th moment always exists.

Property 3: When the mixed noise approaches Gaussian noise, the model can be simplified as

$$f_{N_m}(n) = \frac{1}{2\sqrt{\pi\gamma_{sg}}} e^{-\frac{n^2}{4\gamma_{sg}}}. \quad (11)$$

Then, we have

$$\alpha = 2, c_1 = 1, c_2 = +\infty, C_\alpha = 0, I = 2g_0\sqrt{\pi\gamma_{sg}}, \quad (12)$$

when the mixed noise degenerates to Gaussian noise.

Similarly, when the mixed noise approaches purely impulsive noise, we have the following property.

Property 4: When the mixed noise approaches to impulsive noise, the model can be simplified as

$$f_{N_m}(n) = \frac{\alpha \gamma_s C_\alpha}{I(|n|^{\alpha+1} + c_2)}, \quad (13)$$

and

$$c_1 = 0, c_2 = \frac{\alpha\gamma_s C_\alpha}{g_0},$$

$$I = 2g_0 c_2^{\frac{1}{\alpha+1}} \Gamma\left(\frac{\alpha}{\alpha+1}\right) \Gamma\left(\frac{\alpha+2}{\alpha+1}\right). \quad (14)$$

Property 5: $f_{N_m}(n) = \mathcal{O}(n^{-\alpha+\eta-1})$, where $\mathcal{O}(\cdot)$ represents the upper bounded function. That is, $\exists N > 0, \alpha > \eta > 0, k > 0, \forall n > N$, we have

$$f_{N_m}(n) \leq \frac{k}{n^{\alpha-\eta+1}}. \quad (15)$$

Property 6: $f_{N_m}(n) = \omega(n^{-\alpha-\delta-1})$, where $\omega(\cdot)$ represents the lower bounded function. That is, $\exists N > 0, \delta > 0, k > 0, \forall n > N$, we have

$$f_{N_m}(n) \geq \frac{k}{n^{\alpha+\delta+1}}. \quad (16)$$

Property 5 and 6 are straightforward because the main lobe decays extremely fast and all the parameters of the tail section are finite.

Remarks: Compared with other noise models, the above mentioned mixed noise model is adopted in this paper for the following reasons:

- 1) There are various scenarios containing the non-gaussian IN [1–3], where the WGN inevitably exists due to the Brownian movement of electrons, which leads to the mixed noise that can be described by (3).
- 2) The model can degenerate to special cases with specific parameters as described by Property 3 and 4, which makes the model able to describe a cluster of noise, i.e., WGN, IN and mixed Gaussian-impulsive noise (MGIN).
- 3) Some parameters in the mixed model have the same mechanism with S α S distribution, i.e. α and γ [17]. Therefore, these parameters can be estimated directly by the methods for S α S noise.

III. CAPACITY-ACHIEVING INPUT DISTRIBUTION

For the MGIN channel, it is rather challenging to obtain explicit channel capacity and the optimal input distribution achieving capacity due to many factors such as complicated PDF expression and the lack of the second moment. In this section, we analyze the capacity of MGIN channel and discuss the characteristics of the optimal input distribution achieving capacity.

We set the power constraint of X to be

$$\mathbb{E}[|X|^p] \leq P_0 < +\infty, \quad (17)$$

where $1 \leq p < \alpha$ to assure the constraint convexity. The lower bound of p is to ensure the constraint is convex. Besides, without loss of generality, we consider the distribution of X to be symmetric which means

$$F_X(x) = 1 - F_X(-x), \forall x \geq 0. \quad (18)$$

where $F_X(x)$ is the probability distribution function of X . We focus on zero-mean mixed noise since the direct current offset can be eliminated by subtracting a constant from the received signals. Thus, it is obvious that the output distribution F_Y should also be symmetric. To conveniently express the distribution function F_X of X , we define $\mathcal{B}(\mathbb{R})$ to be the Borel σ -algebra generated by \mathbb{R} which represents the real number set. We define the set of distribution functions Ω to be

$$\Omega = \left\{ F_X \left| \int_{-\infty}^{+\infty} |x|^p dF_X \leq P_0, F_X(x) = 1 - F_X(-x), \forall x \in \mathbb{R}, 1 \leq p < \alpha \right. \right\}. \quad (19)$$

Therefore, the capacity can be expressed as

$$C(X, Y) = \sup_{F_X \in \Omega} I(F_X) = \sup_{F_X \in \Omega} [h(Y) - h(Y|X)], \quad (20)$$

where ‘ $I(\cdot)$ ’ and ‘ $h(\cdot)$ ’ denote mutual information and entropy, respectively. We apply $I(F_X)$ instead of $I(Y; X)$ because the channel model and the mutual information will be determined by F_X .

In what follows, we first analyze the existence of $h(Y)$ and $h(Y|X)$. Then, we discuss the existence and uniqueness of $C(X, Y)$, and present the characteristics of capacity-achieving distribution.

A. Existence of $h(Y)$ and $h(Y|X)$

If $h(Y)$ and $h(Y|X)$ are both finite, they will exist. Before analyzing the bounds of $h(Y)$ and $h(Y|X)$, we first propose a useful lemma relating to the constraint (17).

Lemma 1: $\mathbb{E}[|Y|^p]$ is finite.

Proof: It follows (1) and (2) that the received signal can be expressed as $Y = X + N_s + N_g$. Thus, according to the Loeve’ Cr inequality [19], we have

$$\mathbb{E}[|Y|^p] \leq C_r (\mathbb{E}[|X|^p] + \mathbb{E}[|N_s|^p] + \mathbb{E}[|N_g|^p]), \quad (21)$$

$$C_r = \begin{cases} 1, & p > 1 \\ 3^{p-1}, & 0 \leq p \leq 1, \end{cases} \quad (22)$$

where N_g and N_s follow Gaussian distribution and S α S distribution, respectively. We denote them as $N_g \sim \mathcal{N}(0, 2\gamma_g^2)$ and $N_s \sim S(\alpha, 0, \gamma_s, 0)$, respectively. As arbitrary p -th moment of N_g exists, $\mathbb{E}[|Y|^p]$ could be bounded to be

$$0 < \mathbb{E}[|Y|^p] \leq P_0 + C_{p,\alpha} + \mathbb{E}[|N_g|^p] < +\infty, \quad (23)$$

where [4]

$$C_{p,\alpha} = \frac{2^{p+1}\Gamma\left(\frac{p+1}{2}\right)\Gamma\left(\frac{-p}{\alpha}\right)}{\alpha\sqrt{\pi}\Gamma\left(\frac{-p}{2}\right)}. \quad (24)$$

Conditional entropy $h(Y|X)$ can be express as

$$h(Y|X) = -\mathbb{E}_{\mu_X} \left[\int_{-\infty}^{+\infty} f_{N_m}(y|x) \log f_{N_m}(y|x) dy \right], \quad (25)$$

where μ_X is the probability measure of X . It has support \mathbb{R} and is defined on $(\mathbb{R}, \mathcal{B}(\mathbb{R}))$. In fact, for every fixed x , the $h(Y|X = x)$ can be transformed to $h(Y|X = 0)$ through variable substitution. Thus, we just need to prove that $h(N_m)$, i.e., $h(Y|X = 0)$, is finite.

Lemma 2: $h(Y)$ and $h(Y|X)$ are both finite.

Proof: The proof of Lemma 2 is provided in Appendix A. ■

B. Existence and Uniqueness of $C(X, Y)$

According to optimization theory, if Ω is weak* compact and the mutual information function is weak* continuous, the capacity will exist. Furthermore, if Ω is also convex and $I(F_X)$ is a strictly concave function in Ω , $C(X, Y)$ will be unique [20].

Lemma 3: Ω is convex and weak* compact.

Proof: The proof of Lemma 3 is relegated to Appendix B. ■

Next, we need to prove that $I(F_X)$ is continuous and strictly concave in Ω . For continuity, we will show both $h(Y|X)$ and $h(Y)$ are weak* continuous. In fact, $h(Y|X)$ is apparently continuous since N_m is purely additive noise and $h(Y|X)$ could be equivalent to $h(N_m)$. Therefore, we just need to show $h(Y)$ is weak* continuous.

Lemma 4: $h(Y)$ is weak* continuous.

Proof: The proof of Lemma 4 is relegated to Appendix C. ■

Meanwhile, based on the (2), the characteristic function (CF) of the N_m should be

$$\phi_{N_m}(t) = \phi_{N_s}(t)\phi_{N_g}(t) = \exp(-\gamma_s|t|^\alpha - \gamma_g t^2). \quad (26)$$

Note that (3) is an approximated PDF for the distribution with the CF in (26). Thus, we assume the CF of (3) with appropriate parameter estimation is just corresponding to the PDF (26). Then, we have $\phi_{N_m}(t) > 0, \forall t \in \mathbb{R}$ and the mutual information function $I(F_X)$ can be demonstrated to be strictly concave by following the similar procedure to prove Theorem 12 in [7] and Levy continuity theorem. Finally, the uniqueness of $C(X, Y)$ can be concluded.

C. Characteristics of Capacity-achieving Input Distribution

In the previous subsection, we conclude that the capacity of MGIN channel exists and is unique. Subsequently, we discuss the characteristics pertaining to capacity-achieving input distribution. We first introduce the KKT condition with respect to capacity-achieving input distribution as it is very difficult to obtain explicit PDF expression.

1) *KKT Condition*: By taking constraint (17) into consideration, the Lagrange function of mutual information is

$$J(F_X, \lambda) = I(F_X) - \lambda \underbrace{\left(\int_{-\infty}^{+\infty} |x|^p dF_X - P_0 \right)}_{\phi(F_X)}, \quad (27)$$

where λ is a non-negative Lagrangian multiplier. Note that $\phi(F_X)$ is a convex constraint due to $p \geq 1$. Meanwhile, the symmetry constraint is not explicitly integrated in (27) as F_X is symmetric by default. Moreover, we can only consider the amplitude of X .

As it has been proved that Ω is a convex set and $I(F_X)$ is concave, Lagrangian theorem is evidently satisfied. Furthermore, if $I(F_X)$ and $\phi(F_X)$ are weakly differentiable, it always holds that $\frac{\partial J(F_X, \lambda)}{\partial F_X} \leq 0$ for $\forall F_X \in \Omega$ and $I(F_X)$ can reach the maximum in Ω at F_X^* and $\frac{\partial J(F_X, \lambda)}{\partial F_X} \Big|_{F_X=F_X^*} = 0$ [6]. Therefore, we need to first show that all parts in (27) are weakly differentiable. We have the following Lemma.

Lemma 5: $I(F_X)$ and $\phi(F_X)$ are weakly differentiable.

Proof: The proof of Lemma 5 is relegated to Appendix D. ■

Consequently, with (27) and (D.6), we have the following inequality,

$$\begin{aligned} \frac{\partial J(F_X, \lambda)}{\partial F_X} &= -\mathbb{E}_{\mu_x} \left[\int_{-\infty}^{+\infty} f_{N_m}(y|x) \log f_Y(y, F_X^*) dy \right] - C \\ &\quad - h(N_m) - \lambda[\phi(F_X) - \phi(F_X^*)] \leq 0, \forall F_X \in \Omega. \end{aligned} \quad (28)$$

Based on Theorem 4 in [6], (28) can be equivalently transformed into

$$\frac{\partial J(x, \lambda)}{\partial x} = \int_{-\infty}^{+\infty} f_{N_m}(y|x) \log f_Y(y, F_X^*) dy + C + h(N_m) + \lambda(|x|^p - P_0) \begin{cases} > 0, \forall x \in \mathbb{R} - \mathcal{S}^* \\ = 0, \forall x \in \mathcal{S}^*, \end{cases} \quad (29)$$

where \mathcal{S}^* indicates the set containing optimal mass points. Actually, the points in \mathcal{S}^* are the mass points of F_X^* in Ω^* and they are completely related. (29) reveals that for given F_X^* , there exists $\lambda > 0$ such that the equality holds if $x \in \mathcal{S}^*$. Furthermore, it is obvious that the Slater's constraint qualification can be satisfied by F_X , which assures F_X^* is optimal if there are Lagrange multipliers satisfying KKT conditions [6].

2) *Characteristics of The Optimal Input*: Subsequently, we prove that the support of optimal F_X is discrete and contains only finite mass points. The basic idea is to make a contradiction based on the assumption that there are infinite points in \mathcal{S}^* . We first extend $J(x, \lambda)$ to complex domain,

$$\frac{\partial J(z, \lambda)}{\partial z} = \underbrace{\int_{-\infty}^{+\infty} f_{N_m}(y|z) \log f_Y(y, F_Z^*) dy}_{\Psi(z)} + \lambda(|z|^p - P_0) + C + h(N_m), z \in \mathcal{C}, \quad (30)$$

where \mathcal{C} denotes complex domain. It follows (3) that the feasible domain of $\frac{\partial J(z, \lambda)}{\partial z}$ is $\Omega_J = \{z \mid |z|^{p+1} + c_2 \neq 0\}$.

Lemma 6: $\frac{\partial J(z, \lambda)}{\partial z}$ is analytic everywhere in Ω_J .

Proof: In fact, the right-hand side (RHS) of (30) except $\Psi(z)$ is obviously analytic, and we only need to prove the integral is also analytic. Equivalently, it is sufficient to verify $\Psi(z)$ is uniformly convergent, i.e., [21]

$$\lim_{k \uparrow +\infty} \int_k^\infty f_{N_m}(y|z) \log f_Y(y, F_Z^*) dy = 0. \quad (31)$$

where $a \uparrow (\downarrow) b$ represents that b is the left (right) limit of a . Based on Property 5, there exists $\alpha > \eta_1 > 0, k_1 > 0, \rho_1 > 0, \forall y > \rho_1$ such that

$$f_{N_m}(y|z) < \frac{k_1}{|y|^{\alpha - \eta_1 + 1}}. \quad (32)$$

Similar to (C.3), we can obtain the upper bound of $f_Y(y, F_Z^*)$, and there exist $k_2 > 0, \eta_2 > 0, \rho_2 > 0, \forall y > \rho_2$ such that

$$f_Y(y, F_Z^*) < \frac{k_2}{|y|^q}, \quad (33)$$

where $q = \min\{\alpha - \eta_2 + 1, p\} \geq 1$. Let $y > \max\{\rho_1, \rho_2\}$, $|f_{N_m}(y|z) \log f_Y(y, F_Z^*)|$ can be bounded by

$$|f_{N_m}(y|z) \log f_Y(y, F_Z^*)| < \frac{k_1(\log k_2 - q \log |y|)}{y^{\alpha - \eta_1 + 1}}. \quad (34)$$

The upper bound in (34) is completely integrable and satisfies (31). ■

Then, we need to verify that the support of optimal input distribution is bounded even though there is no peak limitation in our problem formulation. Let $T(n)$ be

$$T(n) = \log \frac{1}{f_{N_m}(n)}. \quad (35)$$

It follows Property (6) that there exist $\delta > 0, c > 0, \forall n > c$ such that

$$T(n) < \log |n|^{\alpha + 1 + \delta} = (\alpha + 1 + \delta) \log |n|. \quad (36)$$

Obviously, we have the constraint $|n|^p = \omega(T(n))$, i.e., $\forall \kappa > 0, \exists c > 0, \forall n > c$ such that $|n|^p \geq \kappa T(n)$. Consequently, according to Theorem 1 in [22], we can conclude that the \mathcal{S}^* is compact. Furthermore, by Weierstrass-Bolzano theorem, there must exist an accumulation in \mathcal{S}^* . KKT condition indicates

that all of them are the zero points of $\frac{\partial J(z,\lambda)}{\partial z}$. Based on the identity theorem of an analytic function, $\frac{\partial J(z,\lambda)}{\partial z}$ always equals zero in the feasible region. However, when z is rather large, (30) could not equal zero except that $\lambda = 0$, which is a contradiction with Lagrangian theorem. Hence, we claim that there are finite mass points in \mathcal{S}^* .

D. Algorithm

It is quite difficult (or even impossible) to obtain the explicit solution of problem (29) due to the complicated integral and mixed noise model. Fortunately, the problem can be parameterized to a vector optimization problem [23] and then, optimization algorithms can be applied to find the solution.

There are three kinds of parameters including the number, position and probability of mass points. Smith has demonstrated the number of mass points will increase monotonically as the SNR becomes larger [23]. Therefore, we can specifically assume that there are two points in \mathcal{S}^* , and denote the position and probability to be x_i and p_i ($i = 1, 2$), respectively. The initialized p_i can be updated by BA-algorithm in [24] when keeping x_i fixed. Then, p_i is fixed and x_i will be updated by the gradient ascent method to maximize the mutual information function. The iteration will be repeated until convergence. Finally, the obtained mass points will be checked whether they satisfy the KKT condition in (29). The number of mass points will increase by one, and the above iteration operation will be repeated if (29) could not be satisfied.

IV. CAPACITY LOWER BOUND

In the previous section, we have proved that the capacity of mixed noise channel exists and is unique. Based on the analysis and numerical methods, we can numerically compute the capacity. However, we could not get closed-form capacity expression. In this section, we derive the analytical capacity lower bounds based on the mutual information. We first propose the model approximation lemma which will be utilized in what follows.

Lemma 7: The mixed noise model in (3) can be approximated as follows,

$$f_{N_m}(n) \approx \hat{f}_{N_m}(n) = \begin{cases} \frac{g_0}{I} e^{-\frac{n^2}{4\gamma_{sg}}}, & |n| < n_0 \\ \frac{\alpha\gamma_s C_\alpha}{I(|n|^{\alpha+1} + c_2)}, & |n| \geq n_0, \end{cases} \quad (37)$$

where n_0 is the intersection of piecewise functions in (37) under Kullback-Leibler Divergence (KLD) minimization criteria.

Proof: As the mixed noise model (3) is the linear combination of two functions, it is extremely challenging to obtain closed-form mutual information due to the log operation. Nevertheless, when n becomes large, the influence of the exponential term can be neglected. Moreover, we can observe that the

two piecewise functions in (3) have similar behaviors when $|n| < n_0$. Therefore, we can only retain the exponential term to approximate the whole mixed noise model in the region. Thus, (37) can be obtained, and the remaining task is to determine the threshold n_0 .

As KLD can measure the difference between two distribution functions [17], we obtain n_0 via minimizing the KLD between $f_{N_m}(n)$ and $\hat{f}_{N_m}(n)$, which is written as

$$\begin{aligned} \mathcal{K} \left[f_{N_m}(n); \hat{f}_{N_m}(n) \right] &= \int_0^{+\infty} f_{N_m}(n) \log \frac{f_{N_m}(n)}{\hat{f}_{N_m}(n)} dn \\ &= \int_0^{+\infty} f_{N_m}(n) \log f_{N_m}(n) dn - \log \frac{g_0}{I} \int_0^{n_0} f_{N_m}(n) dn \\ &\quad + \frac{1}{4\gamma_{sg}} \int_0^{n_0} n^2 f_{N_m}(n) dn + \int_{n_0}^{+\infty} f_{N_m}(n) \log \frac{I}{\alpha\gamma_s C_\alpha} \\ &\quad + \int_{n_0}^{+\infty} f_{N_m}(n) \log (|n|^{\alpha+1} + c_2) dn. \end{aligned} \quad (38)$$

As $f_{N_m}(n)$ and $\hat{f}_{N_m}(n)$ are both symmetric, we only consider the non-negative part. Obviously, $\mathcal{K} \left[f_{N_m}(n); \hat{f}_{N_m}(n) \right]$ is convex with respect to n_0 . Then, we have

$$\frac{\partial \mathcal{K}}{\partial n_0} = \left(-\log \frac{g_0}{I} + \frac{n_0^2}{4\gamma_{sg}} \right) f_{N_m}(n_0) - \left[\log(|n|^{\alpha+1} + c_2) + \log \frac{g_0}{\alpha\gamma_s C_\alpha} \right] f_{N_m}(n_0). \quad (39)$$

By setting it to zero, we can get

$$\frac{\partial \mathcal{K}}{\partial n_0} = 0 \Rightarrow \frac{\alpha\gamma_s C_\alpha}{g_0 (|n_0|^{\alpha+1} + c_2)} = e^{-\frac{n_0^2}{4\gamma_{sg}}}. \quad (40)$$

The optimal n_0 can then be obtained by solving the above equation numerically. ■

With the aid of Lemma 7, $h(N_m)$ can be easily computed. Moreover, this lemma indicates that the approximated noise model is still continuous.

A. Lower Bound L_1

In this subsection, we find a capacity lower bound based on the mutual information. We set $f_X(x)$ to be a distribution so that the resulting $f_Y(y)$ can be easily handled. Let X follow the same distribution with N_m , i.e., the distribution of X is given as follows,

$$f_{N_m}(x) = \frac{g_{x0}}{I_x} \left[c_{x1} e^{-\frac{x^2}{4\gamma_{xsg}}} + \frac{c_{x2}(1 - c_{x1})}{|x|^{\alpha+1} + c_{x2}} \right], \quad (41)$$

where the additional subscript x is added in these parameters to avoid notational confusion. The similar operation is also applied in what follows. Then, we will show Y have the same distribution as N_m . According to (2), X and Y can be expressed as

$$X = X_g + X_s, \quad (42)$$

$$Y = Y_g + Y_s = (X_g + N_g) + (X_s + N_s), \quad (43)$$

where both X_g and N_g follow Gaussian distribution, and both X_s and N_s follow S α S distribution. We denote $X_g \sim \mathcal{N}(0, 2\gamma_{xg}^2)$, $N_g \sim \mathcal{N}(0, 2\gamma_{ng}^2)$, $X_s \sim S(\alpha, 0, \gamma_{xs}, 0)$ and $N_s \sim S(\alpha, 0, \gamma_{ns}, 0)$, respectively. Based on the additive property of Gaussian distribution and S α S distribution [16], we can get $Y_g \sim \mathcal{N}(0, 2\gamma_{yg}^2)$ and $Y_s \sim S(\alpha, 0, \gamma_{ys}, 0)$. Then we can conclude Y also follows the mixed noise model with $\gamma_{yg} = (\gamma_{xg}^2 + \gamma_{ng}^2)^{1/2}$ and $\gamma_{ys} = (\gamma_{xs}^\alpha + \gamma_{ns}^\alpha)^{1/\alpha}$. c_{y1} and γ_{ysg} can be estimated based on the empirical methods presented in [17].

Finally, it follows mutual information and Lemma 7 that the lower bound of capacity can be given as

$$C \geq h(Y) - h(N_m) \triangleq L_1. \quad (44)$$

The detailed derivation can be found in Appendix E.

B. Lower Bound L_2

In this subsection, we further present a closed-form lower bound based on the maximum entropy theorem [5], which can be expressed as follows,

$$C \geq \frac{1}{2} \log \left(1 + e^{2[h(X) - h(N_m)]} \right) \triangleq L_2. \quad (45)$$

Thus, we can get a tighter lower bound by maximizing $h(X)$. According to the maximum entropy theorem, the optimal $f_X(x)$ under input constraints should be [5]

$$f_X(x) = e^{\lambda_0 + \lambda_1 |x|^p}, \forall x \in \mathbb{R}. \quad (46)$$

Meanwhile, $f_X(x)$ has to satisfy the following constraints,

$$\int_{-\infty}^{+\infty} f_X(x) dx = 1, \quad (47)$$

$$\int_{-\infty}^{+\infty} |x|^p f_X(x) dx = P_0. \quad (48)$$

Then, we can get

$$\lambda_0 = \frac{p-1}{p} \log p - \frac{1}{p} \log P_0 - \log [2\Gamma(1/p)], \quad (49)$$

$$\lambda_1 = -\frac{1}{pP_0}, \quad (50)$$

$$h(X) = -\lambda_0 + \frac{1}{p}. \quad (51)$$

Therefore, the capacity lower bound can be obtained. Note that $h(N_m)$ can be calculated by following Appendix E.

C. Asymptotic Performance of Lower Bound

When the mixed noise channel is very close to Gaussian channel, the parameters of the mixed noise model follow Property 3. Therefore, we have

$$\lim_{c_{y1} \uparrow 1} h(Y) = -\frac{g_{y0}}{I_y} \left[y_0 e^{-\frac{y_0^2}{4\gamma_{ysg}}} + \left(2 \log \frac{g_{y0}}{I_y} - 1 \right) \sqrt{\pi\gamma_{ysg}} \times \mathcal{F} \left(\frac{y_0}{2\sqrt{\gamma_{ysg}}} \right) \right], \quad (52)$$

where $\mathcal{F}(\cdot)$ is the Gaussian error function and $\mathcal{F}(z) = \frac{2}{\sqrt{\pi}} \int_0^z e^{-t^2} dt$. Recall the definition of y_0 , we have $\lim_{c_{y1} \uparrow 1} y_0 = +\infty$ since the tail section becomes zero and the intersection will be reached when $y \rightarrow +\infty$. In that case,

$$\lim_{c_{y1} \uparrow 1, c_{y2} \uparrow +\infty} h(Y) = -\frac{g_{y0}}{I_y} \sqrt{\pi\gamma_{ysg}} \left(2 \log \frac{g_{y0}}{I_y} - 1 \right) = \frac{1}{2} \log 4\pi e\gamma_{ysg}. \quad (53)$$

Therefore, we can derive the bounds from (44) for WGN,

$$C \geq \frac{1}{2} \log \frac{\gamma_{ysg}}{\gamma_{nsg}}, \quad (54)$$

where γ_{ysg} denotes the variance for this case. γ_{ysg} is also additive, i.e., $\gamma_{ysg} = \gamma_{nsg} + \gamma_{xsg}$. Then, (54) could be $C \geq \frac{1}{2} \log (1 + \gamma_{xsg}/\gamma_{nsg}) = \frac{1}{2} \log (1 + P_X/P_N)$. In this case, p can be 2 since the finite variance exists, and the bound will be certainly Shannon capacity. In fact, the equality can be reached because the optimal input is the Gaussian distributed.

For L_2 , when MGIN turns to WGN and p converges to α , the distribution will be Gaussian distribution. Based on the additive property of normal distribution, Y is also a Gaussian RV and L_2 will degenerate to Shannon formula. The analysis indicates the generality of the two lower bounds. Note that when MGIN degenerates to IN, the approximation of (44) will introduce a large error, and y_0 will converge to 0. However, the similar capacity lower bounds can be calculated directly based on Property 4. As the resulting expressions are rather complicated, we omit them in this paper.

V. CAPACITY UPPER BOUND

We analyze upper bounds with the duality expression of capacity. In [8], the discrete duality inequality based on relative entropy was provided and it was extended to continuous form which is equivalent to an infinite input alphabet. The generalized upper bound is expressed as

$$C \leq \mathbb{E}_{\mu_x} \left[\mathcal{D} \left(\hat{f}_{N_m}(y|x); f_R(y) \right) \right], \quad (55)$$

where $\mathcal{D} \left(\hat{f}_{N_m}(y|x); f_R(y) \right)$ represents relative entropy which is

$$\mathcal{D} \left(\hat{f}_{N_m}(y|x); f_R(y) \right) = \int_{-\infty}^{+\infty} \hat{f}_{N_m}(y|x) \log \frac{\hat{f}_{N_m}(y|x)}{f_R(y)} dy, \quad (56)$$

and the $f_R(y)$ is an arbitrary output distribution to generate the upper bound and the equality will reach when $f_R(y) = f_Y(y)$ [8]. An elaborated $f_R(y)$ will lead to a tight upper bound with closed forms. In

this section, we will derive two capacity upper bounds with different output distributions. For convenient expression, we still utilize parameters in (37) to represent the distribution of N_m in the following.

A. Upper Bound U_1

The first upper bound U_1 will be given by the following theorem.

Theorem 1: Let the arbitrary output distribution $f_R(y)$ to be

$$f_R(y) = \frac{p}{2\Gamma(1/p)} \sigma_1^{-\frac{1}{p}} e^{-\frac{|y|^p}{\sigma_1}}, \forall y \in \mathbb{R}, \sigma_1 > 0, \quad (57)$$

where σ_1 is the parameter of $f_R(y)$. Then, the capacity upper bound is

$$C \leq \frac{1}{p} (1 + \log \sigma_1^*) + \log \frac{2\Gamma(1/p)}{p} - h(N_m), \quad (58)$$

where σ_1^* is the best choice of σ_1 and

$$\sigma_1^* = p(P_0 + \mathbb{E}[|N_m|^p]). \quad (59)$$

Proof: Based on (55), we can obtain that

$$\begin{aligned} C &\leq \inf_{\sigma_1} \left\{ \mathbb{E}_{\mu_x} \left[\mathcal{D} \left(\hat{f}_{N_m}(y|x); f_R(y) \right) \right] \right\} \\ &= \inf_{\sigma_1} \left\{ -\mathbb{E}_{\mu_x} \left[\int_{-\infty}^{+\infty} \hat{f}_{N_m}(y|x) \log f_R(y) dy \right] - h(N_m) \right\}. \end{aligned} \quad (60)$$

Plugging (57) into (60),

$$\begin{aligned} -\mathbb{E}_{\mu_x} \left[\int_{-\infty}^{+\infty} \hat{f}_{N_m}(y|x) \log f_R(y) dy \right] &= -\mathbb{E}_{\mu_x} \left[\int_{-\infty}^{+\infty} \hat{f}_{N_m}(y|x) \left(\log \tilde{K}_1 - \frac{|y|^p}{\sigma_1} \right) dy \right] \\ &\stackrel{(a)}{=} -\log \tilde{K}_1 + \frac{1}{\sigma_1} \mathbb{E}_{\mu_x} \left[\int_{-\infty}^{+\infty} \hat{f}_{N_m}(z) |x + z|^p dz \right] \\ &\stackrel{(b)}{\leq} -\log \tilde{K}_1 + \frac{1}{\sigma_1} \mathbb{E}_{\mu_x} \left[\int_{-\infty}^{+\infty} \hat{f}_{N_m}(z) (|x|^p + |z|^p) dz \right] \\ &= -\log \tilde{K}_1 + \frac{1}{\sigma_1} (\mathbb{E}[|N_m|^p] + \mathbb{E}_{\mu_x}[|X|^p]) \\ &\stackrel{(c)}{\leq} -\log \tilde{K}_1 + \frac{1}{\sigma_1} \underbrace{(\mathbb{E}[|N_m|^p] + P_0)}_{\tilde{K}_2}, \end{aligned} \quad (61)$$

where we denote \tilde{K}_1 as

$$\tilde{K}_1 = \frac{p}{2\Gamma(1/p)} \sigma_1^{-\frac{1}{p}}. \quad (62)$$

In (61), (a) is from the variable substitution $z = y - x$ and (b) is based on the absolute inequality. (c) is due to the power constraint of input. Therefore, (60) can be further written as

$$C \leq \underbrace{\inf_{\sigma_1} \left\{ -\log \tilde{K}_1 + \frac{\tilde{K}_2}{\sigma_1} - h(N_m) \right\}}_{\tilde{U}_1}. \quad (63)$$

The best σ_1 can be determined from the first derivative of \hat{U}_1 . Note that $h(N_m)$ and \tilde{K}_2 are not related with σ_1 ,

$$\left. \frac{\partial \hat{U}_1}{\partial \sigma_1} \right|_{\sigma_1=\sigma_1^*} = 0 \Rightarrow \sigma_1^* = p(P_0 + \mathbb{E}[|N_m|^p]). \quad (64)$$

After some replacement and simplification, the first capacity upper bound will be (58). ■

With the similar analysis of the asymptotic performance of lower bounds, U_1 can also converge to Shannon formula when MGIN degenerates to WGN.

B. Upper Bound U_2

The second upper bound U_2 will be given by the following theorem.

Theorem 2: Let the arbitrary output distribution $f_R(y)$ to be

$$f_R(y) = \frac{1}{2G(+\infty; 0, p-1, \sigma_2^{-1}) (\sigma_2|y|^p + 1)}, \forall y \in \mathbb{R},$$

$$\sigma_2 > 0, \quad (65)$$

where σ_2 is the parameter of $f_R(y)$. Then, the capacity upper bound will be

$$C \leq \log \frac{2pG(+\infty; 0, p-1, \tilde{K}_2(p-1))}{p-1} - h(N_m), \quad (66)$$

Proof: For the sake of convenience, we denote $G_\infty = G(+\infty; 0, p-1, \sigma_2^{-1})$. Similar to (60), we can obtain the following bound expression,

$$C \leq \inf_{\sigma_2} \left\{ -\mathbb{E}_{\mu_x} \left[\int_{-\infty}^{+\infty} \hat{f}_{N_m}(y|x) \log f_R(y) dy \right] - h(N_m) \right\}. \quad (67)$$

Plugging (65) into (67),

$$\begin{aligned} -\mathbb{E}_{\mu_x} \left[\int_{-\infty}^{+\infty} \hat{f}_{N_m}(y|x) \log f_R(y) dy \right] &= \mathbb{E}_{\mu_x} \left[\int_{-\infty}^{+\infty} \hat{f}_{N_m}(y|x) \log [2G_\infty (\sigma_2|y|^p + 1)] dy \right] \\ &\stackrel{(a)}{\leq} \log \left\{ 2G_\infty \mathbb{E}_{\mu_x} \left[\int_{-\infty}^{+\infty} \hat{f}_{N_m}(y|x) (\sigma_2|y|^p + 1) dy \right] \right\} \\ &= \log \left\{ 2G_\infty \mathbb{E}_{\mu_x} \left[\int_{-\infty}^{+\infty} \hat{f}_{N_m}(z) (\sigma_2|x + z|^p + 1) dz \right] \right\} \\ &\stackrel{(b)}{\leq} \log \left\{ 2G_\infty \mathbb{E}_{\mu_x} \left[\int_{-\infty}^{+\infty} \hat{f}_{N_m}(z) [\sigma_2(|x|^p + |z|^p) + 1] dz \right] \right\} \\ &= \log \left\{ \underbrace{2G_\infty [\sigma_2(P_0 + \mathbb{E}[|N_m|^p]) + 1]}_{\hat{U}_2} \right\}. \end{aligned} \quad (68)$$

In (68), (a) is based on Jensen inequality and (b) is due to the triangle inequality. The hyperparameters can be determined by the first derivative of \hat{U}_2 . Here, we can obtain that

$$\begin{aligned} \frac{\partial \hat{U}_2}{\partial \sigma_2} &= \lim_{x \rightarrow +\infty} \frac{\partial}{\partial \sigma_2} \left\{ 2G(x; 0, p-1, \sigma_2^{-1}) \left(\sigma_2 \tilde{K}_2 + 1 \right) \right\} \\ &= \lim_{x \rightarrow +\infty} \left\{ \frac{1 + \sigma_2 \tilde{K}_2}{p\sigma_2} \frac{x}{1 + \sigma_2 x^p} + \left(\tilde{K}_2 - \frac{1 + \sigma_2 \tilde{K}_2}{p\sigma_2} \right) \times G(x; 0, p-1, \sigma_2^{-1}) \right\} \\ &= \left(\tilde{K}_2 - \frac{1 + \sigma_2 \tilde{K}_2}{p\sigma_2} \right) G(+\infty; 0, p-1, \sigma_2^{-1}). \end{aligned} \quad (69)$$

Based on (69),

$$\frac{\partial \hat{U}_2}{\partial \sigma_2} = 0 \Rightarrow \sigma_2^* = \frac{1}{\tilde{K}_2(p-1)}, \quad (70)$$

where we have $G(+\infty; 0, p-1, \sigma_2^{-1}) > 0$. Thus, plugging (68) and (70) into (67) will lead to the second capacity upper bound. ■

VI. CAPACITY RELATING TO MODULATION SCHEME

In practice, it is valuable to discuss the achievable channel capacity with regard to specific modulation schemes. In this section, we further consider the capacity of M -array pulse amplitude modulation (M-PAM) under additive MGIN. Note that the M^2 -array QAM constellation can be considered as two symmetric M-PAM modulated constellations. For instance, We have $C_{16QAM} = 2C_{4PAM}$ and consequently, we take the capacity of 4-PAM modulation as an example in what follows. Obviously, we can still employ BA algorithm to obtain the corresponding capacity. To facilitate calculating, we derive concise closed-form expressions. We only consider the lower bound herein based on mutual information function, and the upper bound can be also established via relative entropy in Section V.

First, the mutual information can be expressed as

$$I(P_X) = - \int_{-\infty}^{+\infty} f_Y(y) \log f_Y(y) dy - h(N_m), \quad (71)$$

where P_X denotes the probability mass function (PMF) of X and $f_Y(y)$ is

$$f_Y(y) = \sum_{j=1}^M p(x_j) f_{N_m}(y|x = x_j), \quad (72)$$

where M is the modulation order and $M = 4$. (71) can not be expressed with closed form due to the complexity of $f_Y(y)$. Therefore, we will resort to Gauss-Hermite quadrature (GHQ) to convert (71) to a closed form. $h(N_m)$ is independent with input distribution and is calculated in Appendix E. $h(Y)$ is expressed as

$$h(Y) = - \int_{-\infty}^{+\infty} f_Y(y) \log f_Y(y) dy \geq - \log \int_{-\infty}^{+\infty} [f_Y(y)]^2 dy, \quad (73)$$

where (73) follows Jensen inequality. The GHQ can be an accurate estimation of infinite integral with the following form if the number of the polynomial terms is adequate,

$$\int_{-\infty}^{+\infty} e^{-x^2} f(x) dx \approx \sum_{j=0}^{N_h} A_j f(\bar{x}_j), \quad (74)$$

where A_j is the weight factors, N_h is the order of polynomials and \bar{x}_j is the zeros of Hermite polynomials which is symmetric about 0 [25]. For general usage, the function $f(x)$ which could not satisfy the form in (74) is transformed as

$$\int_{-\infty}^{+\infty} f(x) dx = \int_{-\infty}^{+\infty} e^{-x^2} [e^{x^2} f(x)] dx. \quad (75)$$

Thus, we can also simplify $I(P_X)$ to

$$I(P_X) \geq -\log \left\{ \sum_{j=0}^N e^{\bar{x}_j^2} [f_Y(\bar{x}_j)]^2 \right\} - h(N_m) \triangleq \hat{L}_1. \quad (76)$$

Besides, we can also utilize Fano inequality to obtain the lower bound of (71). First, we define a RV V with the PMF to be $f_V(v) = P_e \delta(v) + (1 - P_e) \delta(v - 1)$ where P_e is the symbol error rate of 4-PAM. Then, Fano inequality is expressed as [5]

$$h(X|Y) \leq h(V) + P_e \log(|X| - 1). \quad (77)$$

Without loss of generality, we can set the input distribution of 4-PAM to be uniform in both probability and space to get a lower bound conveniently. Consequently, for mixed channel, P_e can be calculated as

$$\begin{aligned} P_e &= \frac{2(M-1)}{M} \int_{\frac{A}{2}}^{+\infty} \hat{f}_{N_m}(n) dn \\ &= \frac{2(M-1)}{M I c_2} \left\{ c_1 c_2 g_0 \sqrt{\pi \gamma_{sg}} \left[1 - \mathcal{F} \left(\frac{A}{4\sqrt{\gamma_{sg}}} \right) \right] + \alpha \gamma_s C_\alpha \left[G(+\infty; \alpha, 0, c_2) - G \left(\frac{A}{2}; \alpha, 0, C_2 \right) \right] \right\}, \end{aligned} \quad (78)$$

where A represents the distance of two adjacent constellation points. Combining with the power constraint, we can get that

$$\frac{2}{M} \sum_{j=1}^{M/2} \left[\frac{A}{2} (2j-1) \right]^p = P_0, \quad (79)$$

and

$$A = \left[\frac{2^{p-1} M P_0}{\sum_{j=1}^{\frac{M}{2}} (2j-1)^p} \right]^{\frac{1}{p}}. \quad (80)$$

Finally, mutual information can be expressed as

$$\begin{aligned} I(P_X) &= h(X) - h(X|Y) \\ &\geq \log M - h(V) - P_e \log(M-1) \\ &= \log M + P_e \log \frac{P_e}{M-1} + (1-P_e) \log(1-P_e) \triangleq \hat{L}_2. \end{aligned} \quad (81)$$

Plugging (78) into (81), we can get the second lower bound \hat{L}_2 . The performance of \hat{L}_1 and \hat{L}_2 will be discussed in the next section.

VII. NUMERICAL RESULTS

In this section, we will first calculate the numerical channel capacity of the mixed noise in various scenarios. Then, we will compare these bounds and capacity with different α to check the tightness of our bounds. Finally, we consider the practical application of the channel capacity with 4-PAM modulation.

A. Numerical Capacity

We apply the algorithm in Section III to obtain the approximate numerical capacity. To use BA algorithm, we need to discretize and truncate the mixed channel. The convergence of the problem conversion has been discussed in [24]. In fact, mixed channel model is similar to $S\alpha S$ channel since the tail sections of PDF are almost the same. Following the procedure in [26] for $S\alpha S$ channel, we can also get that the truncation loss is $\mathcal{O}(n_T^{-\alpha})$ where n_T is the truncation point. In order to decrease the error, n_T should be as large as possible and we set the range of n in $f_{N_m}(n)$ to be $|n| \leq n_T$ and $n_T = \min\{n_r | \int_{-n_r}^{n_r} f_{N_m}(n)dn > 0.99\}$. Note that n_T will increase rapidly when both α and generalized signal-to-noise ratio (GSNR) are quite small. Besides, when the GSNR becomes very large, the whole PDF will concentrate in a rather limited range. Thus, the stepsize of X-axis is set to 0.01 to assure the accuracy of the model. Then, due to the lack of variance, we define the GSNR to be

$$GSNR(dB) = 10 \log_{10} \frac{\mathbb{E}[|X|^p]}{\mathbb{E}[|N_m|^p]}, \quad (82)$$

where p can be any value that is less than α and for example, p can be set to $\alpha - 0.1$. However, when we want to compare the influence of α on the capacity, different values of p will have the capacity curves with different slopes because P_0 is fixed. Therefore, we set $p = \min(I_\alpha) - 0.1$ where I_α is the set containing all α used in simulation. Besides, we also consider the cases for which the channel degenerates to a purely impulsive channel and Gaussian channel to check the generality of the results. The numerical capacities for different values of α are shown in Fig. 2. It shows that the capacity becomes larger when α is closer to 2 and the Gaussian special case has the largest capacity, which is consistent with analysis. Meanwhile, the capacity of $S\alpha S$ distributed purely impulsive noise is the lowest one, which verifies that the channel capacity decreases when the impulsivity of noise is more considerable.

B. Comparison of Capacity and Bounds

We simulate the capacity bounds with different α . Note that all of the bounds contain parameters of the mixed noise model which need to be estimated. We apply the ECF based method to obtain their

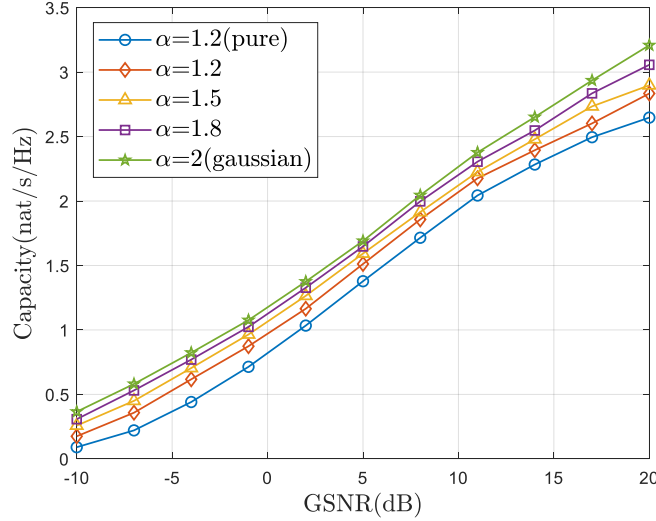
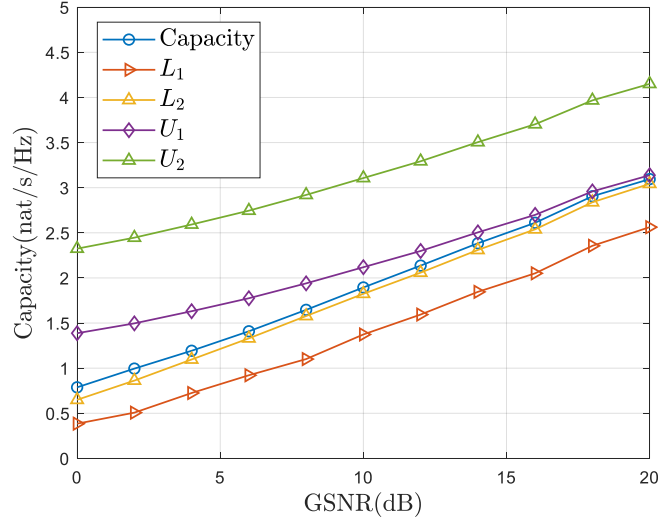
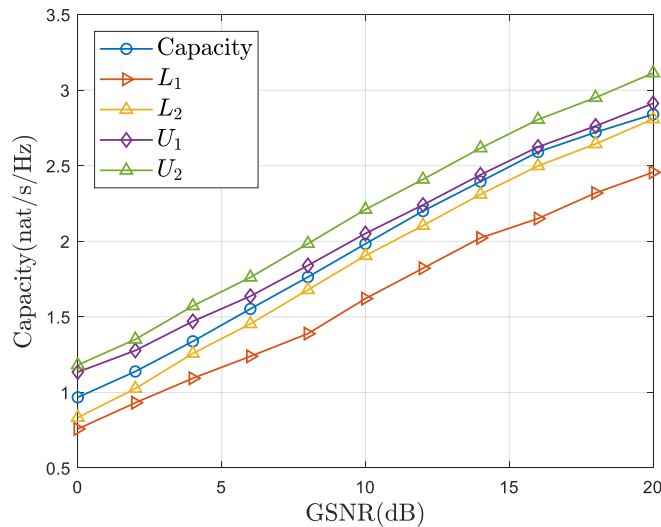


Fig. 2: Numerical capacity with different values of α ($p=1.1$)

estimates with mixed noise samples. Therefore, the estimation error will introduce jitter to the bounds. In order to reduce the variance of the curve and make it more smooth, we take the average over 10 epochs. We choose $\alpha = 1.2$ and $\alpha = 1.8$ to be the simulation scenarios with different impulsivity. The mixed noise with $\alpha = 1.8$ is close to WGN, which has a larger capacity. Corresponding capacities and bounds are shown in Fig. 3 and 4. Note that all of the bounds have the same slope with capacity and the L_2 is very tight in both scenarios. The gap between the capacity and L_2 is only 0.1 nats when GSNR reaches 20dB. The asymptotic behavior of the capacity, L_2 and U_1 are quite similar, which coincides with the derivations and analyses in Section IV and V. U_1 is generally tighter than U_2 , and U_2 is also tight when the impulsivity of mixed noise is smaller. The reason is the output corresponding to the optimal input distribution is not heavy and therefore, U_1 is tighter than U_2 because the (57) is more suitable for the output distribution .

C. Capacity under 4-PAM Modulation

The capacity under modulation order constraint with different values of α is shown in Fig. 5. Compared with the curves in Fig. 2, the capacity upper limit can be observed since a symbol under 4-PAM modulation can represent at most 2 bits. Similar to the channel capacity without modulation order constraint, to reach the same bit error rate (BER) performance, the smaller α is, the larger the required GSNR is. The capacity with different α will approach 2 bit/s/Hz when $\text{GSNR} \rightarrow +\infty$. However, the capacity becomes stable when GSNR is larger than 25dB, which demonstrates that the capacity improvement for communication systems is slight through increasing the GSNR when it is large enough.


 Fig. 3: Capacity and bounds when $\alpha = 1.2$

 Fig. 4: Capacity and bounds when $\alpha = 1.8$

Finally, the capacity and its lower bounds are compared in Fig. 6. To assure the accuracy of GHQ, we choose the order of polynomials N_h to be 30. Note that the number of polynomial terms N_h used in GHQ increases when GSNR becomes too large, e.g., 30dB. In that case, $f_Y(y)$ is similar to the linear combination of delta function which is difficult for GHQ to produce a reasonable estimation. For instance, to retain the estimation accuracy, we need to have $N_h \geq 50$ if GSNR continues to increase. The bound based on the Fano's inequality is more accurate when GSNR is larger and P_e is smaller. Note that when $P_e \rightarrow 0$, \hat{L}_2 becomes $\log M$ which is the capacity limit of M-PAM. In other words, the bound in (81) can

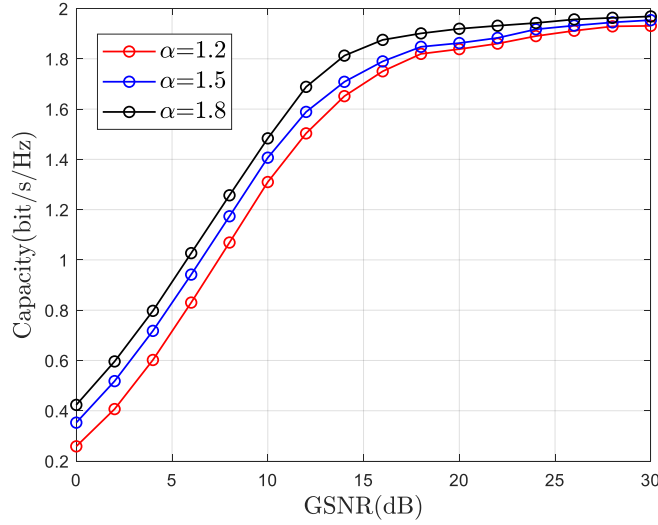


Fig. 5: Capacity of 4-PAM with different α

converge to capacity when GSNR is large enough. The results demonstrate that the mutual information is rather tight with the capacity, especially when GSNR is relatively large. It means that the equiprobable and equispaced constellation is an effective choice in MGIN channel.

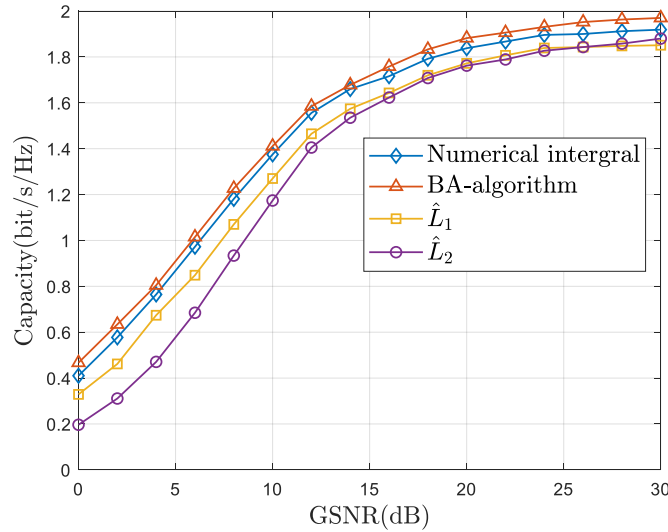


Fig. 6: Capacity and lower bounds of 4-PAM when $\alpha = 1.5$

VIII. CONCLUSION

In this paper, we addressed the capacity and capacity bounds of the MGIN channel. The MGIN channel model and some pertinent properties were first given. Then, we theoretically proved the existence and

uniqueness of the capacity and derived the KKT condition of the resulting optimization problem. Moreover, we demonstrated that the optimal input contains only finite mass points. For practical applications, concise and closed-form lower and upper bounds of the capacity were given. Theoretical analysis showed that the lower bounds can degrade to Shannon formula when MGIN becomes WGN. We also considered the capacity for 4-PAM modulation scheme under MGIN channel and proposed 2 lower bounds based on quadrature and Fano's inequality. Experimental results showed that the capacity is related with α , and our bounds were tight particularly when α and GSNR were large. In addition, uniform constellation was shown to be efficient for modulation under the MGIN channel.

APPENDIX A
PROOF OF LEMMA 2

$h(N_m)$ can be written as

$$h(N_m) = -2 \left[\underbrace{\int_0^{\delta_1} f_{N_m}(n) \log f_{N_m}(n) dn}_{W_0} + \underbrace{\int_{\delta_1}^{+\infty} f_{N_m}(n) \log f_{N_m}(n) dn}_{W_1} \right], \quad (\text{A.1})$$

where $\delta_1 = \min\{\delta_0 | f_{N_m}(\delta_0) \leq 1, \delta_0 > 0\}$ and therefore, $W_1 < 0$. Furthermore, with Property 6, $-W_1$ can be bounded as

$$\begin{aligned} - \int_{\delta_1}^{+\infty} f_{N_m}(n) \log f_{N_m}(n) dn &< - \int_{\delta_1}^{+\infty} f_{N_m}(n) \log \frac{k}{n^{\alpha+\delta+1}} dn \\ &= \int_{\delta_1}^{+\infty} f_{N_m}(n) [-\log k + (\alpha + \delta + 1) \log n] dn \\ &< \max\{-\log k, 0\} + (\alpha + \delta + 1) \int_{\delta_1}^{+\infty} f_{N_m}(n) \log n dn \\ &< \max\{-\log k, 0\} + (\alpha + \delta + 1) \int_{\delta_1}^{+\infty} \frac{k \log n}{n^{\alpha-\eta+1}} dn \\ &< +\infty. \end{aligned} \quad (\text{A.2})$$

Meanwhile, as we have $f_{N_m}(n) \leq g_0/I$, W_0 is definitely finite. Therefore, we can conclude that $h(Y|X)$ exists.

For $h(Y)$, it is obvious that $\exists N > 0, \forall n > N$ such that $f_Y(n) < 1$ and $\lim_{n \uparrow +\infty} f_Y(n) = 0$. Similarly, we can also get that $h(Y)$ is lower bounded by finite value. The upper bound of $h(Y)$ can be given by Gibbs' inequality. We further define the following PDF,

$$g(y) = \frac{p}{2\Gamma(1/p)} e^{-|y|^p}, \forall y \in \mathbb{R}. \quad (\text{A.3})$$

Then, we have

$$\begin{aligned}
 - \int_{-\infty}^{+\infty} f_Y(y) \log f_Y(y) dy &\stackrel{(a)}{\leq} - \int_{-\infty}^{+\infty} f_Y(y) \log g(y) dy \\
 &= \mathbb{E} [|Y|^p] \log \frac{p}{2\Gamma(1/p)} \\
 &\stackrel{(b)}{<} +\infty.
 \end{aligned} \tag{A.4}$$

The (a) is based on the non-negativity of relative entropy and (b) is from (23). Therefore, $h(Y)$ is also finite.

APPENDIX B

PROOF OF LEMMA 3

For convexity, we define $f_X(x) = \theta f_{X_1}(x) + (1 - \theta) f_{X_2}(x)$, $\theta \in (0, 1)$ and f_{X_1} and f_{X_2} both belong to Ω . Then we have

$$\begin{aligned}
 \int_{-\infty}^{+\infty} |x|^p f_X(x) dx &= \int_{-\infty}^{+\infty} |x|^p [\theta f_{X_1}(x) + (1 - \theta) f_{X_2}(x)] dx \\
 &= \theta \mathbb{E} [|X|^p; F_{X_1}] + (1 - \theta) \mathbb{E} [|X|^p; F_{X_2}] \\
 &\leq \theta P_0 + (1 - \theta) P_0 = P_0.
 \end{aligned} \tag{B.1}$$

Besides, it is clear that $f_X(x)$ is symmetric if both of $f_{X_1}(x)$ and $f_{X_2}(x)$ are symmetric. Therefore, $f_X(x)$ is still in Ω , which implies the set is convex.

To prove the weak* compactness of Ω , we first show that Ω is tight, which means that $\forall \epsilon > 0$, there $\exists L > 0$ such that [6]

$$\sup_{F_X \in \Omega} 1 - F_X(L) < \epsilon, \tag{B.2}$$

where F_X is the distribution function of f_X . In fact, $\mathbb{E} [|X|^p]$ is finite and we have

$$\begin{aligned}
 \mathbb{E} [|X|^p] &= 2 \left[\int_0^L |x|^p f_X(x) dx + \int_L^{+\infty} |x|^p f_X(x) dx \right] \\
 &\geq 2 \left(\tilde{M} + L^p [1 - F(L)] \right),
 \end{aligned} \tag{B.3}$$

where $\tilde{M} \triangleq \int_0^L |x|^p f_X(x) dx$. Therefore, we can get

$$0 < 1 - F(L) \leq \frac{\mathbb{E} [|X|^p] - 2\tilde{M}}{2L^p} \leq \frac{P_0 - 2\tilde{M}}{2L^p}. \tag{B.4}$$

Then, we need to obtain an upper bound with analytic expression of $-\tilde{M}$ to assure (B.2), which is equivalent to finding a finite upper bound for $\int_L^{+\infty} |x|^p f_X(x) dx$. Actually, for $\forall L_t > 0$,

$$\int_{L_t}^{+\infty} |x|^p f_X(x) dx < \frac{P_0}{2}. \tag{B.5}$$

Based on the power constraint, it is straightforward that the decay order of $f_X(x)$ should be larger than $p + 1$, i.e., $f_X(x) = \mathcal{O}(|x|^{-(p+1)})$. We assume that there exists a finite $L \geq L_t > 0, r > 0$ such that $f_X(x) \leq k/x^{p+r+1}$ if $x \geq L_t$. Combing with (B.5), we can get that $k \leq P_0 r L_t^r / 2$ and

$$\begin{aligned} \int_L^{+\infty} |x|^p f_X(x) dx &\leq \int_{L_t}^{+\infty} |x|^p f_X(x) dx \\ &\leq \int_L^{+\infty} |x|^p \frac{P_0 r L_t^r}{2x^{p+1+r}} dx \\ &= \frac{P_0 L_t^r}{2L^r}, L \geq L_t. \end{aligned} \tag{B.6}$$

Then,

$$-\tilde{M} = - \left[\frac{P_0}{2} - \int_L^{+\infty} |x|^p f_X(x) dx \right] \leq \frac{P_0}{2} \left(\frac{L_t^r}{L^r} - 1 \right), \tag{B.7}$$

$$\frac{P_0 - 2\tilde{M}}{2L^p} \leq \frac{P_0 L_t^r}{2L^{r+p}} < \epsilon. \tag{B.8}$$

Let finite L to be larger than $\max\{L_t, (P_0 L_t^r / 2\epsilon)^{1/(r+p)}\}$ and then, we can conclude Ω is tight. [6] indicates that Ω is also relatively compact based on Prokhorov's theorem which means for every function sequence $\{F_n\}$ in Ω , there always exists a subsequence $\{F_{n_k}\}$ such that

$$F_{n_k} \xrightarrow{w^*} F^*. \tag{B.9}$$

If F^* also belongs to Ω , then Ω will be sequentially compact and compact. In fact, the distribution function and probability measure is bijection [27]. So there exists measure sequences μ_{n_k} such that $\mu_{n_k} \xrightarrow{w^*} \mu^*$. Obviously, F^* follows the symmetric property in (18). Combining with continuous and bounded below function $|x|^p$, we have [19]

$$\int_{-\infty}^{+\infty} |x|^p \mu^*(dx) \leq \lim_{n_k \uparrow +\infty} \int_{-\infty}^{+\infty} |x|^p \mu_{n_k}(dx) \leq P_0. \tag{B.10}$$

Hence, F^* is still in the Ω .

APPENDIX C

PROOF OF LEMMA 4

We first present the following Proposition.

Proposition 1: $|x \log x| < \frac{2}{1-r} x^r, 0 < x < 1, 0 < r < 1$.

Proof: When $0 < x < 1$, $|x \log x| = -x \log x$. We define function $g(x) = 2x^r / (1-r) + x \log x$. Therefore, we can verify that $g(x)$ is convex when $x \in (0, 1)$ based on the first and second partial derivatives of $g(x)$. Consequently, it is straightforward that $g(x)$ reaches minimum when $\frac{\partial g(x)}{\partial x} = 0$ and we can get $\min\{g(x)\} = 2x^{r-1} - 1 > 0$. ■

The PDF of received signal $f_Y(y)$ can be expressed as

$$f_Y(y) = \int_{-\infty}^{+\infty} f_{N_m}(y|x) dF_X. \quad (\text{C.1})$$

From (3), we get that $f_Y(y) < g_0/I$. Based on (17), we have

$$\int_{-\infty}^{+\infty} |x|^p f_X(x) dx \leq P_0 < +\infty. \quad (\text{C.2})$$

Combining with Property 5 and decay order of $f_X(x)$, we have $y > y_t > 0$ such that

$$\begin{aligned} f_Y(y) &= 2 \left[\int_0^{y_t} f_{N_m}(y|x) dF_X + \int_{y_t}^{+\infty} f_{N_m}(y|x) dF_X \right] \\ &\leq 2 \left[\int_0^{y_t} \frac{k_2}{y^{\alpha+1-\eta}} dF_X + \int_{y_t}^{+\infty} f_{N_m}(y|x) dF_X \right] \\ &\leq 2 \left[\int_0^{y_t} \frac{k_2}{y^{\alpha+1-\eta}} dF_X + \frac{g_0}{I} \int_{y_t}^{+\infty} dF_X \right] \\ &\leq 2 \left[\frac{k_2}{y^{\alpha+1-\eta}} \int_{-\infty}^{+\infty} dF_X + \frac{g_0}{I} \int_{y_t}^{+\infty} \frac{k_1}{x^{p+1}} dx \right] \\ &= \frac{2k_2}{y^{\alpha+1-\eta}} + \frac{2g_0k_1}{y_t^p I p}, \end{aligned} \quad (\text{C.3})$$

where $\alpha > \eta$ and we assume y_t satisfying $\mathcal{Q}(y_t) = 0.5$. Note that $y > y_t$ aims to assure that k_2 is finite.

Obviously, there exists $1 < b < +\infty$ and $y = by_t$ and then,

$$f_Y(y) \leq \frac{2k_2}{y^{\alpha+1-\eta}} + \frac{2g_0k_1}{(by)^p I p} \triangleq \mathcal{Q}(y) \leq \frac{1}{2}, y > y_t. \quad (\text{C.4})$$

Furthermore, we define $\chi_Y(y)$ to be

$$\chi_Y(y) = \begin{cases} \frac{g_0}{I}, 0 \leq y < y_t \\ \max \left\{ \frac{4k_2}{y^{\alpha+1-\eta}}, \frac{4g_0k_1}{(by)^p I p} \right\} \leq 1, y \geq y_t. \end{cases} \quad (\text{C.5})$$

Note that the $\chi_Y(y), y \geq y_t$ should be less than 1 to satisfy the domain of the function in Proposition

1. Therefore, based on the Proposition 1, the dominated function of $|f_Y(y) \log f_Y(y)|$ can be

$$\chi(y) = \begin{cases} \frac{g_0}{I} \log \frac{g_0}{I}, 0 \leq y < y_t \\ \frac{2}{1-r} \max \left\{ \left(\frac{4k_2}{y^{\alpha+1-\eta}} \right)^r, \left[\frac{4g_0k_1}{(by)^p I p} \right]^r \right\}, y \geq y_t. \end{cases} \quad (\text{C.6})$$

Obviously, when we choose $\max \{r(\alpha + 1 - \eta), rp\} > 1$, $\chi(y)$ is still absolutely integrable along the real number line and then, the dominated function can be established. Hence, based on the dominated convergence theorem [28],

$$\begin{aligned} \lim_{n \uparrow +\infty} h(Y, F_{Y_n}) &= - \lim_{n \uparrow +\infty} \int_{-\infty}^{+\infty} f_{Y_n}(y) \log f_{Y_n}(y) dy \\ &= - \int_{-\infty}^{+\infty} \lim_{n \uparrow +\infty} f_{Y_n}(y) \log f_{Y_n}(y) dy \\ &= h(Y, F_Y). \end{aligned} \quad (\text{C.7})$$

It means that $h(Y)$ is weak* continuous over F_Y .

APPENDIX D

PROOF OF LEMMA 5

$I(F_X)$ is weakly differentiable iff

$$\frac{I_{F_{X_0}}(F_X)}{\partial F_X} = \lim_{\epsilon \downarrow 0} \frac{I[(1-\epsilon)F_{X_0} + \epsilon F_X] - I(F_{X_0})}{\epsilon} \quad (\text{D.1})$$

exists for all $F_X \in \Omega$. Let $F_X^\epsilon = (1-\epsilon)F_X^* + \epsilon F_X$, and the PDF of output corresponding to F_X^ϵ follows linearity. That is

$$f_Y(y, F_X^\epsilon) = (1-\epsilon)f_Y(y, F_X^*) + \epsilon f_Y(y, F_X). \quad (\text{D.2})$$

Then, we have

$$\begin{aligned} I(F_X^\epsilon) - I(F_X^*) &= - \int_{-\infty}^{+\infty} [(1-\epsilon)f_Y(y, F_X^*) + \epsilon f_Y(y, F_X)] \log f_Y(y, F_X^\epsilon) dy \\ &\quad + \int_{-\infty}^{+\infty} f_Y(y, F_X^*) \log f_Y(y, F_X^*) dy \\ &= \epsilon \int_{-\infty}^{+\infty} [f_Y(y, F_X^*) - f_Y(y, F_X)] \log f_Y(y, F_X^\epsilon) dy \\ &\quad + \int_{-\infty}^{+\infty} f_Y(y, F_X^*) \log \frac{f_Y(y, F_X^*)}{f_Y(y, F_X^\epsilon)} dy. \end{aligned} \quad (\text{D.3})$$

Therefore, according to definition of (D.1), we can get

$$\begin{aligned} \frac{\partial I_{F_X^*}(F_X)}{\partial F_X} &= \lim_{\epsilon \downarrow 0} \frac{I(F_X^\epsilon) - I(F_X^*)}{\epsilon} \\ &= \lim_{\epsilon \downarrow 0} \left[\int_{-\infty}^{+\infty} f_Y(y, F_X^*) \log f_Y(y, F_X^*) dy - \int_{-\infty}^{+\infty} f_Y(y, F_X) \log f_Y(y, F_X^*) dy \right. \\ &\quad \left. + \frac{1}{\epsilon} \int_{-\infty}^{+\infty} f_Y(y, F_X^*) \log \frac{f_Y(y, F_X^*)}{f_Y(y, F_X^\epsilon)} dy \right], \end{aligned} \quad (\text{D.4})$$

where the third term of (D.4) can be proved to be zero when $\epsilon \rightarrow 0$. In fact,

$$\begin{aligned} \lim_{\epsilon \downarrow 0} \frac{1}{\epsilon} \int_{-\infty}^{+\infty} f_Y(y, F_X^*) \log \frac{f_Y(y, F_X^*)}{f_Y(y, F_X^\epsilon)} dy &= \lim_{\epsilon \downarrow 0} \int_{-\infty}^{+\infty} \frac{1}{\epsilon} f_Y(y, F_X^*) \times \\ &\quad \log \frac{f_Y(y, F_X^*)}{(1-\epsilon)f_Y(y, F_X^*) + \epsilon f_Y(y, F_X)} dy \\ &= \lim_{\epsilon \downarrow 0} \int_{-\infty}^{+\infty} f_Y(y, F_X^*) \log \left[\frac{1}{1-\epsilon + \epsilon \Delta} \right]^{\frac{1}{\epsilon}} dy \\ &= \lim_{\epsilon \downarrow 0} \int_{-\infty}^{+\infty} f_Y(y, F_X^*) \log \left[1 + \frac{\epsilon - \epsilon \Delta}{1-\epsilon + \epsilon \Delta} \right]^{\frac{1}{\epsilon}} dy \\ &= \lim_{\epsilon \downarrow 0} \int_{-\infty}^{+\infty} f_Y(y, F_X^*) \log e^{\frac{1-\Delta}{1-\epsilon + \epsilon \Delta}} dy \\ &= \int_{-\infty}^{+\infty} f_Y(y, F_X^*) (1-\Delta) dy = 0, \end{aligned} \quad (\text{D.5})$$

where $\Delta = f_Y(y, F_X)/f_Y(y, F_X^*)$. Note that we have $I(F_X^*) = C$, $\phi(F_X^*) = 0$ and consequently,

$$\begin{aligned} \frac{\partial I_{F_X^*}(F_X)}{\partial F_X} &= \int_{-\infty}^{+\infty} f_Y(y, F_X^*) \log f_Y(y, F_X^*) dy \\ &\quad - \int_{-\infty}^{+\infty} f_Y(y, F_X) \log f_Y(y, F_X^*) dy \\ &= - \int_{-\infty}^{+\infty} f_Y(y, F_X) \log f_Y(y, F_X^*) dy - C \\ &\quad - h(N_m). \end{aligned} \tag{D.6}$$

Furthermore, it is trivial that $\phi(F_X)$ is also weakly differentiable and

$$\frac{\partial \phi_{F_X^*}(F_X)}{\partial F_X} = \phi(F_X) - \phi(F_X^*) = \phi(F_X). \tag{D.7}$$

APPENDIX E

DERIVATION OF L_1

We represent the capacity with mutual information, i.e.,

$$C \geq I(F_X) = h(Y) - h(N_m). \tag{E.1}$$

Note that we only need to calculate $h(Y)$ as both Y and N_m follow the mixed noise model with the same α . It follows Lemma 7 that $h(Y)$ can be expressed as

$$\begin{aligned} h(Y) &\approx -2 \int_0^{+\infty} \hat{f}_{N_m}(y) \log \hat{f}_{N_m}(y) dy \\ &= -2 \int_0^{y_0} \frac{g_{y0}}{I_y} e^{-\frac{y^2}{4\gamma_{ysg}}} \log \frac{g_{y0}}{I_y} e^{-\frac{y^2}{4\gamma_{ysg}}} dy - 2 \underbrace{\int_{y_0}^{+\infty} \frac{\alpha\gamma_{ys}C_\alpha}{I_y(y^{\alpha+1} + c_{y2})} \log \frac{\alpha\gamma_{ys}C_\alpha}{I_y(y^{\alpha+1} + c_{y2})} dy}_{L_1^*} \\ &= -\frac{2g_{y0}}{I_y} \int_0^{y_0} \left(\log \frac{g_{y0}}{I_y} - \frac{y^2}{4\gamma_{ysg}} \right) e^{-\frac{y^2}{4\gamma_{ysg}}} dy - 2L_1^* \\ &= -\frac{g_{y0}}{I_y} \left[y_0 e^{-\frac{y_0^2}{4\gamma_{ysg}}} + \left(2 \log \frac{g_{y0}}{I_y} - 1 \right) \sqrt{\pi\gamma_{ysg}} \times \mathcal{F} \left(\frac{y_0}{2\sqrt{\gamma_{ysg}}} \right) \right] - 2L_1^*. \end{aligned} \tag{E.2}$$

Note that $\mathcal{F}(z) = \frac{2}{\sqrt{\pi}} \int_0^z e^{-t^2} dt$ and C_α is only related with α . (E.2) admits closed-form expression by variable substitution. We first divide the L_1^* into two parts,

$$\begin{aligned} L_1^* &= \int_{y_0}^{+\infty} \frac{\alpha\gamma_{ys}C_\alpha}{I_y(y^{\alpha+1} + c_{y2})} \log \frac{\alpha\gamma_{ys}C_\alpha}{I_y} dy - \underbrace{\int_{y_0}^{+\infty} \frac{\alpha\gamma_{ys}C_\alpha}{I_y(y^{\alpha+1} + c_{y2})} \log (y^{\alpha+1} + c_{y2}) dy}_{L_1^{**}} \\ &= \frac{\alpha\gamma_{ys}C_\alpha}{I_y c_{y2}} [G(+\infty; \alpha, 0, c_{y2}) - G(y_0; \alpha, 0, c_{y2})] \log \frac{\alpha\gamma_{ys}C_\alpha}{I_y} - L_1^{**}. \end{aligned} \tag{E.3}$$

The last equation follows formula (8). Let $u = y^{\alpha+1} + c_{y2}$, L_1^{**} can then be represented as

$$L_1^{**} = \frac{\alpha\gamma_{ys}C_\alpha}{I_y(\alpha+1)} \int_{\kappa_y}^{+\infty} (u - c_{y2})^{-\frac{\alpha}{\alpha+1}} \frac{\log u}{u} du, \tag{E.4}$$

where we denote $\kappa_y = y_0^{\alpha+1} + c_{y2}$. Before proceeding, we first introduce the following integration formula [18],

$$\int \frac{\log x}{x(x-b)^a} dx = -\frac{x^{-a}}{a^2} \left[\tilde{G}(x, a, b) + aG_1(x, a, b) \log x \right] \\ \triangleq W(x, a, b), a > 0, b > 0, \quad (\text{E.5})$$

where

$$\tilde{G}(x, a, b) = \tilde{H}_g \left(\{a, a, a\}, \{1+a, 1+a\}, \frac{b}{x} \right), \quad (\text{E.6})$$

$$G_1(x, a, b) = H_g \left(a, a, 1+a, \frac{b}{x} \right), \quad (\text{E.7})$$

and \tilde{H}_g represents the generalized hypergeometric function. It is trivial to get $\tilde{G}(+\infty, a, b) = G_1(+\infty, a, b) =$

1. Therefore, we have $W(+\infty, a, b) = 0$. By following these formulas, we can get

$$L_1^{**} = \frac{\alpha\gamma_{ys}C_\alpha}{I_y\alpha^2} \kappa_y^{-\frac{\alpha}{\alpha+1}} \left[(\alpha+1)\tilde{G} \left(\kappa_y, \frac{\alpha}{\alpha+1}, c_{y2} \right) + \alpha G_1 \left(\kappa_y, \frac{\alpha}{\alpha+1}, c_{y2} \right) \log \kappa_y \right]. \quad (\text{E.8})$$

Finally, $h(Y)$ could be expressed as

$$h(Y) \approx -\frac{g_{y0}}{I_y} \left[y_0 e^{-\frac{y_0^2}{4\gamma_{ys}g}} + \left(2 \log \frac{g_{y0}}{I_y} - 1 \right) \sqrt{\pi\gamma_{ys}g} \mathcal{F} \left(\frac{y_0}{2\sqrt{\gamma_{ys}g}} \right) \right] - \frac{2\alpha\gamma_{ys}C_\alpha}{I_y c_{y2}} [G(+\infty; \alpha, 0, c_{y2}) \\ - G(y_0; \alpha, 0, c_{y2})] \log \frac{\alpha\gamma_{ys}C_\alpha}{I_y} + \frac{2\alpha\gamma_{ys}C_\alpha}{I_y\alpha^2} \kappa_y^{-\frac{\alpha}{\alpha+1}} \left[(\alpha+1)\tilde{G} \left(\kappa_y, \frac{\alpha}{\alpha+1}, c_{y2} \right) + \alpha G_1 \left(\kappa_y, \frac{\alpha}{\alpha+1}, c_{y2} \right) \log \kappa_y \right] \quad (\text{E.9})$$

Meanwhile, $h(N_m)$ could be similarly expressed by substituting the corresponding parameters. Then, we can get the lower bound in (44).

REFERENCES

- [1] U. Epple and M. Schnell, "Advanced blanking nonlinearity for mitigating impulsive interference in ofdm systems," *IEEE Trans. Veh. Technol.*, vol. 66, no. 1, pp. 146–158, 2017.
- [2] P. Chen, Y. Rong, S. Nordholm, Z. He, and A. J. Duncan, "Joint channel estimation and impulsive noise mitigation in underwater acoustic ofdm communication systems," *IEEE Trans. Wireless Commun.*, vol. 16, no. 9, pp. 6165–6178, 2017.
- [3] M. Zimmermann and K. Dostert, "Analysis and modeling of impulsive noise in broad-band powerline communications," *IEEE Trans. Electromagn. Compat.*, vol. 44, no. 1, pp. 249–258, 2002.
- [4] M. Shao and C. Nikias, "Signal processing with fractional lower order moments: stable processes and their applications," *Proc. IEEE Proc. IRE**, vol. 81, no. 7, pp. 986–1010, 1993.
- [5] T. M. Cover and J. A. Thomas, *Elements of Information Theory*. John Wiley & Sons, Ltd, 2005. [Online]. Available: <https://onlinelibrary.wiley.com/doi/pdf/10.1002/047174882X.ch4>
- [6] I. Abou-Faycal, M. Trott, and S. Shamai, "The capacity of discrete-time memoryless rayleigh-fading channels," *IEEE Trans. Inf. Theory*, vol. 47, no. 4, pp. 1290–1301, 2001.
- [7] H. Li, S. M. Moser, and D. Guo, "Capacity of the memoryless additive inverse gaussian noise channel," *IEEE J. Sel. Areas Commun.*, vol. 32, no. 12, pp. 2315–2329, 2014.

- [8] A. Lapidoth and S. Moser, “Capacity bounds via duality with applications to multiple-antenna systems on flat-fading channels,” *IEEE Trans. Inf. Theory*, vol. 49, no. 10, pp. 2426–2467, 2003.
- [9] A. Lapidoth, S. M. Moser, and M. A. Wigger, “On the capacity of free-space optical intensity channels,” *IEEE Trans. Inf. Theory*, vol. 55, no. 10, pp. 4449–4461, 2009.
- [10] A. Lapidoth, J. H. Shapiro, V. Venkatesan, and L. Wang, “The discrete-time poisson channel at low input powers,” *IEEE Trans. Inf. Theory*, vol. 57, no. 6, pp. 3260–3272, 2011.
- [11] J. Wang, E. E. Kuruoglu, and T. Zhou, “Alpha-stable channel capacity,” *IEEE Commun. Lett.*, vol. 15, no. 10, pp. 1107–1109, 2011.
- [12] M. L. de Freitas, M. Egan, L. Clavier, A. Goupil, G. W. Peters, and N. Azzaoui, “Capacity bounds for additive symmetric α -stable noise channels,” *IEEE Trans. Inf. Theory*, vol. 63, no. 8, pp. 5115–5123, 2017.
- [13] M. He, S. Lu, G. Song, J. Cheng, and Y. Watanabe, “Channel capacity with superposed m-pam modulation,” in *2011 Fourth International Conference on Intelligent Computation Technology and Automation*, vol. 2, 2011, pp. 475–478.
- [14] G. Cai, L. Wang, and T. Huang, “Channel capacity of m-ary differential chaos shift keying modulation over awgn channel,” in *2013 13th International Symposium on Communications and Information Technologies (ISCIT)*, 2013, pp. 91–95.
- [15] P. Yang, Y. Wu, and H. Yang, “Capacity of nakagami- m fading channel with bpsk/qpsk modulations,” *IEEE Commun. Lett.*, vol. 21, no. 3, pp. 564–567, 2017.
- [16] G. Samorodnitsky and M. S. Taqqu, *Stable Non-Gaussian Random Processes: Stochastic Models with Infinite Variance*. New York: Chapman & Hall, 1994.
- [17] G. Sureka and K. Kiasaleh, “Sub-optimum receiver architecture for awgn channel with symmetric alpha-stable interference,” *IEEE Trans. Commun.*, vol. 61, no. 5, pp. 1926–1935, 2013.
- [18] D. Zwillinger, V. Moll, I. Gradshteyn, and I. Ryzhik, Eds., *Table of Integrals, Series, and Products (Eighth Edition)*. Boston: Academic Press, 2014.
- [19] Z. Lin and Z. Bai, *Probability Inequalities*. Beijing: Science Press, 2010.
- [20] S. Boyd and L. Vandenberghe, *Convex Optimization*. Cambridge: Cambridge University Press, 2004.
- [21] S. Lang, *Complex Analysis*. New York: Springer-Verlag, 1985.
- [22] J. Fahs and I. Abou-Faycal, “On properties of the support of capacity-achieving distributions for additive noise channel models with input cost constraints,” *IEEE Trans. Inf. Theory*, vol. 64, no. 2, pp. 1178–1198, 2018.
- [23] J. G. Smith, “The information capacity of amplitude- and variance-constrained scalar gaussian channels,” *Inf. Control.*, vol. 18, no. 3, pp. 203–219, 1971.
- [24] R. Blahut, “Computation of channel capacity and rate-distortion functions,” *IEEE Trans. Inf. Theory*, vol. 18, no. 4, pp. 460–473, 1972.
- [25] F. Olver, D. Lozier, R. Boisvert, and C. Clark, *NIST Handbook of Mathematical Functions*. New York: Cambridge University Press, 2010.
- [26] M. Egan, S. M. Perlaza, and V. Kungurtsev, “Capacity sensitivity in additive non-gaussian noise channels,” in *2017 IEEE International Symposium on Information Theory (ISIT)*, 2017, pp. 416–420.
- [27] L. Breiman, *Probability*. Society for Industrial and Applied Mathematics, 1992. [Online]. Available: <https://epubs.siam.org/doi/abs/10.1137/1.9781611971286>
- [28] W. Rudin, *Principles of Mathematical Analysis*. New York, USA: McGraw-Hill, 1964.